Pergamon

Int. J. Solids Structures Vol. 35, Nos 34–35, pp. 4685–4707, 1998

Printed in Great Britain
0020–7683/98/$—see front matter

PII: S0020–7683(98)00090–0

MODELLING THE EFFECT OF FLUID COMMUNICATION ON VELOCITIES IN ANISOTROPIC POROUS ROCKS

SHIYU XU†
Research School of Geological and Geophysical Sciences, Birkbeck and University Colleges, University of London, London WC1E 6BT, U.K.

(*Received* 25 *April* 1997; *in revised form* 29 *January* 1998)

Abstract—An inclusion-based anisotropic poroelasticity model (IBAPM) has been developed from the J. D. Eshelby (1957, *Proceedings of the Royal Society of London Series A*, **241**, 376–396) and T. Mura (1987, *Micromechanics of Defects in Solids*, Martinus Nijhoff, Dordrecht) theories. Eshelby's interaction energy approach is employed to calculate the effective elastic constants of a solid containing dilute pores, since it offers two approximations: one corresponding to the condition of constant load and the other to the condition of constant displacement.

The effect of pore fluid communication on the poroelasticity of a porous rock is modelled via pore connectivity. A totally isolated pore system implies that pore pressure is equilibrated within each individual pore only and may vary from pore to pore, depending on the shape and orientation of each pore. In terms of the local flow mechanism, this gives us a high-frequency estimate of the effective elastic moduli. The low-frequency estimate, on the other hand, is modelled by a communicating pore system. In this case all pores are assumed to be connected and, consequently, pore pressure is equilibrated within the whole pore system.

Other related problems discussed in the paper include: (1) extension of the model to the case of pores having arbitrary orientations, (2) extension of the non-interacting model to higher pore concentrations and (3) consistency checks of IBAPM with previous models. In particular the low-frequency version of the model is compared with the anisotropic version of the Gassmann model (R. J. S. Brown and J. Korringa, 1975, *Geophysics*, **40**, 608–616). Finally the model is applied to the laboratory measurements reported by J. S. Rathore, E. Ejaer, R. M. Holt and L. Renlie (1995, *Geophys. Prosp.*, **43**, 711–728).

1. INTRODUCTION

It is well-known that elastic-wave velocities are frequency dependent. Considerable understanding on the mechanisms of velocity dispersion has been gained from comprehensive laboratory measurements (e.g. Wyllie *et al.*, 1962; Gordon and Davis, 1968; Toksöz *et al.*, 1979; Winkler and Nur, 1982) and theoretical studies (e.g. Gassmann, 1951; Biot, 1956a, b; Walsh, 1966; Mavko and Nur, 1975; O'Connell and Budiansky, 1977). The proposed mechanisms for intrinsic velocity dispersion and, hence, wave attenuation include: (1) local and macro fluid flow (Gassmann, 1951; Biot, 1956a, b; Mavko and Nur, 1975; O'Connell and Budiansky, 1977; White, 1975; Dutta and Odé, 1979a, b) and (2) frictional sliding (Walsh, 1966; Johnston *et al.*, 1979). Since fluid flow mechanisms are considered the main cause of velocity dispersion in sedimentary rocks, they have received considerable attention from research scientists.

Gassmann (1951) proposed a model which simulates elastic bulk and shear moduli of a porous medium containing a totally relaxed pore fluid. Later Biot (1956a, b) developed a comprehensive theory for simulating elastic-wave propagation in fluid-saturated porous media. The Biot–Gassmann (BG) theory has been used to simulate the observed velocity dispersion and wave attenuation of well-consolidated and cemented rocks. In cases where compliant pores (e.g. micro-cracks) are present, however, the BG theory was found to underestimate the velocity dispersion (e.g. Mavko and Jizba, 1994). The extra velocity dispersion was frequently explained as a result of the local fluid flow between compliant and stiff pores.

† Tel.: 0171 187 7050 X2380. Fax: 0171 383 0008. E-mail: xu@geophysics.bbk.ac.uk

The idea of local flow (also called squirt flow) was first proposed by Mavko and Nur (1975). O'Connell and Budiansky (1977) systematically analyzed the problem and proposed a crack model for simulating the effect of local fluid flow on the poroelasticity of a solid containing randomly oriented cracks. Endres and Knight (1997) recently extended the model to a more general case where a solid is permeated with randomly oriented inclusions of arbitrary aspect ratios. Thomsen (1995) took a step further and presented an anisotropic poroelasticity theory applicable to a composite containing two groups of pores: equant inter-granular pores and perfectly aligned thin microcracks.

Xu and White (1995a, b, 1996) treat the problem in a different manner. They employ inclusion-based models (e.g. Kuster and Toksöz, 1974) to calculate the dry rock frame moduli (assuming a zero bulk modulus for the pore fluid at this stage). The differential effective medium (DEM) theory is incorporated into the model to overcome the limitation of dilute pore concentration in these theories. They argue that in dry rock it does not matter if the pores are connected or isolated, since pore pressure is zero. They then use Gassmann's equations to calculate the saturated moduli, implying that all pores are connected and pore pressure is equalized. To model wave velocities at high frequencies, the authors set aside Gassmann's theory and calculate the saturated elastic moduli by including the bulk modulus of the pore fluid when applying the Kuster–Toksöz and DEM theories. A similar approach was also proposed by Ravalec and Gueguen (1996).

Most poroelasticity models (e.g. Gassmann, 1951; Brown and Korringa, 1975; Biot 1956a, b; Mavko and Jizba, 1991, 1994; Mukerji and Mavko, 1994) require the dry bulk and shear moduli as input parameters. This does not cause a serious problem for simulating laboratory measurements, since the dry rockframe moduli can be measured in the laboratory. When constructing seismic models from well logs, however, the dry rockframe moduli are not practically "measurable". The inclusion-based poroelasticity models (e.g. Mavko and Nur, 1975; O'Connell and Budiansky, 1977; Endres and Knight, 1997), on the other hand, predict the effect of the local fluid flow on the poroelasticity of a porous rock from pore parameters. The main advantage of inclusion-based models is that they allow us to study the effect of each individual pore on the poroelasticity. Unfortunately the inclusion-based poroelasticity models mentioned above are restricted to composites having randomly oriented pores. Although Thomsen (1995) developed an anisotropic poroelasticity model, it is limited to a special case where the composite is permeated with two groups of pores: (1) equant pores and (2) perfectly aligned thin cracks. There is considerable potential application for a poroelasticity model applicable to rocks having arbitrary pore orientations and arbitrary aspect ratios.

In this paper, an inclusion-based anisotropic poroelasticity model (IBAPM) is presented. Following the work by O'Connell and Budiansky (1977) and Endres and Knight (1997), two special cases are considered, one corresponding to the isolated pore system and the other to the communicating (undrained) pore system. Numerical examples are then given to demonstrate the impact of pore fluid communication on the poroelasticity of a porous rock. Other related problems, such as the extension of the non-interacting model to higher pore concentrations and consistencies between the IBAPM and previous models, are also discussed. Finally the model is applied to simulate the laboratory measurements reported by Rathore *et al.* (1995).

2. THE CONCEPT OF EIGENSTRAIN AND ITS DETERMINATION

The eigenstrain ε^* is a generic name given to such non-elastic strains, such as thermal expansion, initial strains and plastic strains (Mura, 1987). It was called the stress-free transformation strain by Eshelby (1957). The determination of the eigenstrain ε^* is the key part of estimating effective elastic constants of a composite. For an isolated pore system, Eshelby (1957) has given formulae for calculating ε^* in an isotropic matrix, whereas Mura (1987) has demonstrated how to calculate ε^* in an anisotropic matrix with hexagonal or orthorhombic symmetry. In this section Mura's formulation for isolated pores is reviewed and the formulation for communicating pores is then derived based on principles similar to those of Mura (1987).

2.1. *ε^* for an isolated pore*

For a solid containing isolated pores (or pores without fluid communication), the pore fluid pressure is equalized within each pore. To a first order approximation, the eigenstrain ε_{ij}^* for a particular pore can be calculated by embedding the pore into the matrix. Let C denote the elastic stiffness tensor of the matrix and C^I that of the pore occupying a subdomain Ω,

$$\frac{x^2}{a^2}+\frac{y^2}{a^2}+\frac{z^2}{c^2}=1 \tag{1}$$

We also define

- the applied stress at infinity: σ_{ij}^0
- the applied strain at infinity: $e_{ij}^0 = A_{ijkl}\sigma_{kl}^0$
- the stress deviation from σ_{ij}^0: σ_{ij}
- the strain deviation from e_{ij}^0: e_{ij}.

Inside the pore, Hooke's law is written as

$$\sigma_{ij}^0+\sigma_{ij} = C_{ijkl}^I(e_{kl}^0+e_{kl}) \tag{2}$$

Imagine now that the following transformation is taking place: the pore is replaced by the solid material. To maintain the total strain within Ω exactly the same as that before the transformation, an extra strain ε^* must be introduced. In this sense, the eigenstrain ε^* is the extra strain caused by the presence of the pore replacing matrix material. According to Eshelby (1957) and Mura (1987), the stress–strain relationship in Ω can also be expressed as

$$\sigma_{ij}^0+\sigma_{ij} = C_{ijkl}(e_{kl}^0+e_{kl}-\varepsilon_{kl}^*) \tag{3}$$

Combining eqns (2) and (3), we have

$$C_{ijkl}^I(e_{kl}^0+e_{kl}) = C_{ijkl}(e_{kl}^0+e_{kl}-\varepsilon_{kl}^*) \tag{4}$$

Eshelby (1957) has shown that, if σ_{ij}^0 is uniform, the strain disturbance e_{kl} inside Ω is also uniform as long as Ω is ellipsoidal. e_{kl} can be related to ε^* using the equation given by Eshelby (1957).

$$e_{kl} = S_{klmn}\varepsilon_{mn}^* \tag{5}$$

where S_{klmn} is referred to as the Eshelby tensor, which depends on pore shape and the elastic properties of the matrix. Eshelby (1957) provides the procedure for calculating S_{klmn} in an isotropic matrix and Lin and Mura (1973) and Mura (1987) for solids having hexagonal or orthorhombic symmetry (see Appendix A for Mura's formulae for a solid having hexagonal symmetry).

Substituting eqns (5) into eqn (4) we have

$$C_{ijkl}^I(e_{kl}^0+S_{klmn}\varepsilon_{mn}^*) = C_{ijkl}(e_{kl}^0+S_{klmn}\varepsilon_{mn}^*-\varepsilon_{kl}^*) \tag{6}$$

Applying the rules given in Appendix B and converting the second rank tensors to 9×1 column vectors and the fourth rank tensors to 9×9 matrices, the eigenstrain for an isolated pore (hereafter we name it ε_{iso}^*) is given by

$$\varepsilon^*_{iso} = [(C-C^I)S-C]^{-1}[C^I-C]e^0 \tag{7}$$

2.2. *ε^* for a communicating pore*

The assumption of a completely isolated pore system is plausible only at high frequencies. In reality, pores in sedimentary rocks are rarely totally isolated. They are often connected by pore throats such as microcracks and grain contacts. At high frequencies, there is no time for fluid to flow from one pore to another and they may behave as "isolated" pores. At low frequencies, on the other hand, pore fluid will have plenty of time to interact and the pore pressure will eventually be equalised. The term "communicating" here means that pore pressure will be equilibrated after the sample is subjected to an external stress. This is the basic assumption made also by Gassmann (1951).

The eigenstrain for a communicating pore depends not only on the compressibility of the current pore but also on the compressibilities of other pores within the system. The relationship between the stress in the pore fluid ($\bar{P} = \sigma^0 + \sigma$) and the eigenstrain for this particular pore is given by eqn (3)

$$\bar{P} = C(e^0 + e - \varepsilon^*) \tag{8}$$

Substituting eqn (5) and $\sigma^0 = Ce^0$ into eqn (8), the eigenstrain can be expressed as a function of the differential stress $\bar{P} - \sigma_0$:

$$\varepsilon^* = [C(S-I)]^{-1}(\bar{P} - \sigma^0) \tag{9}$$

There are, in general, two ways of estimating the pore stress change $\bar{P}_{ij}$ as a function of the applied stress or strain field. The first is to estimate the stress field in each pore and then average it over all pores. Since the total strain in each pore is $e^0 + e$, the average pore stress $\bar{P}$ is

$$\bar{P} = \sum_{n=1}^{N} v_n C^I(e^0 + e) \tag{10}$$

where v_n is the fractional volume of the nth pore normalized by the total pore volume. Thus, we have the relationship

$$\sum_{n=1}^{N} v_n = 1 \tag{11}$$

Gassmann (1951) and Brown and Korringa (1975), on the other hand, have shown that pore pressure, p_f, can also be calculated from the total change in pore volume. Mathematically this can be written as

$$p_f = -k_f \frac{\Delta V_p}{V_p} \tag{12}$$

where k_f is the bulk modulus of the pore fluid and $\Delta V_p / V_p$ is the normalized pore volume change (or dilatation) which can be expressed as a function of the total strain,

$$\frac{\Delta V_p}{V_p} = \sum_{n=1}^{N} v_n \{e^0_{11} + e^0_{22} + e^0_{33} + e_{11} + e_{22} + e_{33}\}_n \tag{13}$$

The pore stresses, $\bar{P}_{ij}$, can then be expressed as a function of pore pressure (Brown and Korringa, 1975),

$$\bar{P}_{ij} = -p_f \delta_{ij} \tag{14}$$

Here δ_{ij} is the Kronecker delta function. Comparing eqns (12)–(14) with eqn (10), it is easy to prove that the pore stresses calculated using the above two schemes are identical. Since the first scheme is much simpler than the second, it will be used in the formulation below.

Substituting eqns (5) and (9) into eqn (10), $\bar{P}$ can be expressed as

$$\bar{P} = C^I e^0 + \sum_{n=1}^{N} v_n C^I S_n [C(S_n - I)]^{-1} (\bar{P} - \sigma^0) \tag{15}$$

which is a function of the geometries of other pores S_n and $\bar{P}$ itself. Noting that both the pore stress $\bar{P}$ and the applied stress σ^0 are constant, the following equation is obtained after some manipulations,

$$\bar{P} = (I - \bar{R})^{-1} (C^I - \bar{R}C) A \sigma^0 \tag{16}$$

where

$$\bar{R} = \sum_{n=1}^{N} v_n R_n \tag{17}$$

and

$$R_n = C^I S_n [C(S_n - I)]^{-1} \tag{18}$$

Equations (16)–(18) show that the pore pressure depends not only on the geometry and orientation of the current pore but also on the geometries and orientations of the other pores within the system. It should be kept in mind, however, the distinction between the interactions of pore fluid and the mechanical interactions between pores. Although the pore fluid pressure is assumed to be equalised, the formulations are valid for dilute pore concentrations only since the mechanical interactions between pores are ignored. Finally the eigenstrain for a communicating pore (hereafter we name it $\varepsilon^*_{\text{com}}$) can be obtained by substituting eqns (16)–(18) into eqn (9),

$$\varepsilon^*_{\text{com}} = [C(S - I)]^{-1} ((I - \bar{R})^{-1} (C^I - \bar{R}C) - C) e^0 \tag{19}$$

3. EFFECTIVE ELASTIC CONSTANTS OF A SOLID WITH DILUTE PORE CONCENTRATIONS

Let us now estimate the effective elastic constants of a solid permeated with dilute ellipsoidal pores having arbitrary aspect ratios and a perfect orientation. The pores are further assumed to be either well-interconnected (communicating) or totally isolated, representing, respectively, the low- and high-frequency cases in terms of the local flow mechanism. In reality, pores in sedimentary rocks are rarely totally isolated. At high frequencies, however, there may be no time for fluid to flow from one pore to another and they may behave as "isolated" pores.

The effective elastic constants of the composite can be approximated by using either the volumetric averaging approach (e.g. Gassmann, 1951; Brown and Korringa, 1975; Hill, 1965; Hornby *et al.*, 1994) or the interaction energy approach (e.g. Eshelby, 1957; Nishizawa, 1982). Both approaches provide identical results as long as the formulation is derived under the same boundary conditions and to the same order of approximation. The interaction energy approach is used here since it offers two approximations yielding, respectively, the upper and lower bounds for the effective elastic constants (Nishizawa, 1982), although the bounds are much wider than the Hashin–Shtrikman (1963) bounds.

Eshelby (1957) has shown that, for a dilute pore concentration, the total energy of the effective medium can be calculated using the following two equations corresponding to two boundary conditions:

1. constant stress applied at infinity

$$\frac{1}{2}A^*_{ijkl}\sigma^0_{ij}\sigma^0_{kl} = \frac{1}{2}A_{ijkl}\sigma^0_{ij}\sigma^0_{kl} + \frac{1}{2}\sum_{n=1}^{N} v_n\sigma^0_{ij}\varepsilon^*_{ij} \tag{20}$$

2. constant strain applied at infinity

$$\frac{1}{2}C^*_{ijkl}e^0_{ij}e^0_{kl} = \frac{1}{2}C_{ijkl}e^0_{ij}e^0_{kl} - \frac{1}{2}\sum_{n=1}^{N} v_nC_{ijkl}e^0_{kl}\varepsilon^*_{ij} \tag{21}$$

Here N denotes the number of pores in the solid; v_n is the volume concentration of the nth pore; C and C^* represent the elastic stiffness tensors of the solid and the effective medium, respectively, and A and A^* denote their corresponding compliance tensors. Following Nishizawa (1982) and above two conditions will hereafter be referred to as the conditions of constant load and constant displacement, respectively.

Nishizawa (1982) has shown how to calculate the effective stiffness and compliance tensors once the eigenstrain ε^* is known. Substituting eqns (7) and (19) into eqns (20) and (21), respectively, we have

$$A^*_{ijkl}\sigma^0_{ij}\sigma^0_{kl} = A_{ijkl}\sigma^0_{ij}\sigma^0_{kl} + \sum_{n=1}^{N} v_n\sigma^0_{ij}Q_{ijkl}A_{klmn}\sigma^0_{mn} \tag{22}$$

for the condition of the constant load, and

$$C^*_{ijkl}e^0_{ij}e^0_{kl} = C_{ijkl}e^0_{ij}e^0_{kl} - \sum_{n=1}^{N} v_nC_{ijkl}e^0_{kl}Q_{ijmn}e^0_{mn} \tag{23}$$

for the condition of the constant displacement. Here

$$Q = [(C-C^I)S-C]^{-1}[C^I-C] \tag{24}$$

for the isolated pores (hereafter referred to as Q_{iso}), and

$$Q = [C(S-I)]^{-1}((I-\bar{R})^{-1}(C^I-\bar{R}C)-C) \tag{25}$$

for communicating pores (hereafter referred to as Q^{com}). Analysis of eqns (7) and (19) reveals that Q is an operator which relates the eigenstrain inside a pore to the applied strain at infinity. It is thus a dimensionless measure of pore compressibility.

Since C is diagonally symmetric, i.e. $C_{ijkl} = C_{klij}$, eqns (22) and (23) may be written as

$$A^*_{ijkl}\sigma^0_{ij}\sigma^0_{kl} = A_{ijkl}\sigma^0_{ij}\sigma^0_{kl} + \sum_{n=1}^{N} v_n[QA]_{ijkl}\sigma^0_{ij}\sigma^0_{kl} \tag{26}$$

and

$$C^*_{ijkl}e^0_{ij}e^0_{kl} = C_{ijkl}e^0_{ij}e^0_{kl} - \sum_{n=1}^{N} v_n[CQ]_{ijkl}e^0_{ij}e^0_{kl} \tag{27}$$

To solve A^*_{1111} from eqn (26), σ^0_{11} is set to one and all the other elements of σ^0 are set to zero. Similarly A^*_{1122} can be obtained by setting σ^0_{11} and σ^0_{22} to one and the other elements

to zero. The same logic can be applied to calculate C^*, but in this case e^0 is varied instead of σ^0.

It must be kept in mind that these equations are valid only for dilute pore concentrations. In the case of isolated pores, Nishizawa (1982) has shown that elastic constants calculated using eqn (26) could differ significantly from those calculated using eqn (27). In fact, eqn (26) gives an upper bound for the effective elastic constants, whereas eqn (27) gives a lower bound. The same may apply to a solid containing communicating pores. Extension of the model to higher pore concentrations will be discussed in detail later.

4. PORE ORIENTATION

The above equations are ready to be applied to a solid containing perfectly aligned pores. In reality, however, pores are often not perfectly aligned but have rather a preferred orientation which may be described, say, by a von Mises distribution. In this section, the model is extended to a more general case of arbitrary orientations of pores.

4.1. *Isolated pores*

In the case of isolated pores, all that is necessary is to calculate $Q^{\text{iso}}A$ in eqn (26) and CQ^{iso} in eqn (27) in a local coordinate system, with the z-axis parallel to the normal of the pore and then transfer them from the local coordinate system to the global coordinate system. Mathematically,

$$[Q^{\text{iso}}A](\theta,\beta)_{ijkl} = T_{ijklmnpq}[Q^{\text{iso}}A]^{\text{local}}_{mnpq} \tag{28}$$

and

$$[CQ^{\text{iso}}](\theta,\beta)_{ijkl} = T_{ijklmnpq}[CQ^{\text{iso}}]^{\text{local}}_{mnpq} \tag{29}$$

where θ is the angle between the global Z-axis and local z-axis and β is the azimuth, the angle between the global X-axis and the projection of the local z on the global XOY plane. $T_{ijklmnpq}$ is the 8th rank transformation tensor which can be calculated using the following equation.

$$T_{ijklmnpq} = K_{im}K_{jn}K_{kp}K_{lq} \tag{30}$$

For oblate spheroidal pores with the same long semi-axis, K_{ij} is represented by the matrix

$$K = \begin{bmatrix} \cos(\theta)\cos(\beta) & -\sin(\beta) & \sin(\theta)\cos(\beta) \\ \cos(\theta)\sin(\beta) & \cos(\beta) & \sin(\theta)\sin(\beta) \\ -\sin(\theta) & 0 & \cos(\theta) \end{bmatrix} \tag{31}$$

4.2. *Communicating pores*

In the case of communicating pores the procedure is more complicated than that for isolated pores. First the tensor R in eqn (17) should be rotated from the local system to the global system, when calculating pore pressure.

$$R(\theta,\beta)_{ijkl} = T_{ijklmnpq}R^{\text{local}}_{mnpq} \tag{32}$$

As shown by eqn (9), the eigenstrain for a communicating pore is the inner product of (a) the compliance of the dry pore $[C(S-I)]^{-1}$ and (b) the differential stress $\bar{P}-\sigma^0$. Under the constant load condition, the differential stress $\bar{P}-\sigma^0$ should remain constant throughout the pore system. It should not, therefore, be rotated. This does not mean that the pore pressure is independent of the pore orientation. Rather, the effect of pore orientation on

the pore fluid pressure has been considered when calculating $\bar{R}$. Therefore, only the term $[C(S-I)]^{-1}$ in eqn (25) needs to be rotated,

$$[C(S-I)]^{-1}(\theta,\beta)_{ijkl} = T_{ijklmnpq}[[C(S-I)]^{-1}]^{\text{local}}_{mnpq} \tag{33}$$

In the case of applied constant displacement, $[CQ^{\text{com}}]$ can be rewritten as

$$CQ^{\text{com}} = [C[C(S-I)]^{-1}C]\{A(I-\bar{R})^{-1}(C^I-\bar{R}C)-I\} \tag{34}$$

where the term $C[C(S-I)]^{-1}C$ represents the stiffness of the dry pore. Term $A(I-\bar{R})^{-1}(C^I-\bar{R}C)-I$ is a dimensionless measure of the differential strain (pore total strain minus the applied strain). In this case, only the term $C[C(S-I)]^{-1}C$ needs rotating; the other term remains unchanged.

$$[C[C(S-I)]^{-1}C](\theta,\beta)_{ijkl} = T_{ijklmnpq}[C[C(S-I)]^{-1}C]^{\text{local}}_{mnpq} \tag{35}$$

Finally we have,

$$Q^{\text{com}}A = [C(S-I)]^{-1}(\theta,\beta)\{[(I-\bar{R})^{-1}(C^I-\bar{R}C)]A-I\} \tag{36}$$

for the condition of constant load, and

$$CQ^{\text{com}} = [C[C(S-I)]^{-1}C](\theta,\beta)\{A(I-\bar{R})^{-1}(C^I-\bar{R}C)-I\} \tag{37}$$

for the condition of constant displacement.

5. HIGHER PORE CONCENTRATIONS

As mentioned earlier, the formulae given above are valid for dilute pore concentrations only. Unrealistic results, such as a negative bulk modulus, may be obtained when the porosity exceeds a certain value. In the case where the solid is permeated randomly oriented pores with a single aspect ratio, Kuster and Toksöz (1974) give the following limit for the pore concentration

$$\frac{\phi}{\alpha} < 1 \tag{38}$$

where ϕ is the porosity, and $\alpha = (c/a)$ is the aspect ratio. The non-interacting theories are hardly practical with this limitation.

Considerable efforts have been made to overcome the problem. The self-consistent (SC) scheme developed by Hill (1965) and Budiansky (1965) makes it possible to calculate the effective elastic constants of a composite at higher pore concentrations. In the SC scheme, pores are embedded into the effective medium which already contains the pores. Although the scheme provides results within the Hashin–Shtrikman bounds (Willis, 1977), it has been criticized for over-estimating the effect of interactions between the pores. Bruner (1976) comments that the SC scheme overestimates the effect of the interactions by unrealistically considering the interaction between a pore and itself.

The differential effective medium (DEM) scheme (Bruner, 1976; Henyey and Pomphrey, 1982), on the other hand, treats the problem in a different manner. To avoid doubling the effect of the interactions, DEM divides the total pore space ϕ into N portions. The pore concentration $\Delta\phi$ ($\Delta\phi = \phi/N$) for each portion is so small that the assumption of dilute concentration is valid. In combination with a non-interacting theory, DEM then introduces the pores into the system step by step. During each iteration, a portion of pores are introduced into the system and the elastic constants of the effective medium are updated.

The resulting effective medium is then used as the host medium of the next iteration. The procedure is repeated until all the pores are introduced into the system.

It should be noted that the actual pore concentration ΔV to be put into the system during each iteration is larger than $\Delta\phi$ (Nishizawa, 1982; Sheng, 1991; Hornby *et al.*, 1994). This is because, when a certain amount of pore space is put into the system, the same volume of the matrix has to be taken out from the system to maintain the unit total volume. As a result, a fraction of the pore space already embedded in the matrix will be taken out, which needs to be compensated for by increasing the pore concentration for the current portion to be embedded:

$$\Delta V = \frac{1}{1-V}\Delta\phi \tag{39}$$

where V denotes the amount of the pore space embedded into the system so far.

Germonovich and Dyskin (1994a, b) developed a Virial (power) Expansion scheme and used it to calculate the effective shear modulus of an isotropic material with parallel cylindrical inclusions. Their results also demonstrate that the differential effective medium scheme gives more accurate results than the self-consistent scheme. This agrees with the conclusion drawn by Bruner (1976).

It should be noted that both the differential effective medium and self-consistent schemes violate the basic assumption on the equalised pore pressure when they are applied to the communicating pore system. This is because the elastic properties of the host medium vary from iteration to iteration, resulting in a varying pore pressure during the calculation. More discussion about this problem will be given later. But the preliminary results show that more research is needed to solve the problem and this is beyond the scope of this paper.

6. NUMERICAL SIMULATIONS AND DISCUSSION

Numerical simulations have been performed to investigate the combined effects of porosity, pore shape, pore orientation and pore pressure communication on the poroelasticity of a porous rock. The solid (background matrix) is assumed to be isotropic with elastic constants $\lambda = 10.6$ GPa, $\mu = 42.4$ GPa and a density of 2.65 g/cm^3. The pore fluid is assumed to have a bulk modulus of 2.25 GPa and a density of 1 g/cm^3. It is further assumed that the total pore space ($\phi = 5\%$) is equally partitioned into two groups. The first group has an aspect ratio of 0.5 and the second group 0.05. Under these assumptions, two special cases have been studied:

- all the pores are aligned perpendicular to the Z-axis and
- the pores in the first group are aligned perpendicular to the Z-axis whereas the normals of the pores in the second group are at an angle of 45° to the Z-axis but are randomly oriented in the XOY plane.

In both cases the resulting effective medium is transversely isotropic. The five elastic constants, compressibility and the constant-displacement bulk modulus (refer to Appendix C for the definition of the compressibility and bulk modulus for an anisotropic medium) are listed in Table 1.

Several interesting points can be drawn from the numerical results.

- The low-frequency (communicating pores) elastic constants are lower than the corresponding high-frequency (isolated pores) ones. This agrees with the results obtained by O'Connell and Budiansky (1977), Endres and Knight (1997). For a communicating pore system, pore fluid will flow from compliant pores to stiff pores as the rock sample is subjected to a compression. Consequently the equilibrated pore pressure of the communicating pore system should be lower than the pressure in the compliant pores but higher than that in the stiff pores of the same system with isolated pores, making the compliant pores more compliant and stiff pores stiffer. Since the overall elastic constants

Table 1. Tabulation of the numerical results. (a) Case 1: all pores are perfectly aligned, (b) Case 2: pores in Group 1 are aligned perpendicular to z-axis but the normals of the pores in Group 2 have an angle of 45° to the Z-axis. Total porosity is 5% equally partitioned between the two groups

		C_{11}	C_{12}	C_{13}	C_{33}	C_{44}	Compres.	CDBM
(a)								
Const. load	LF	89.54	10.06	8.47	61.41	30.39	0.0316	32.726
	HF	89.55	10.07	8.64	64.29	30.39	0.0309	33.123
	DRY	89.22	9.75	7.05	55.04	30.39	0.0338	31.246
Const. disp.	LF	89.11	10.00	7.45	42.47	25.64	0.0376	30.057
	HF	89.13	10.02	7.82	49.15	25.64	0.0350	30.972
	DRY	88.62	9.51	4.56	25.39	25.64	0.0533	26.656
(b)								
Const. load	LF	79.07	9.43	9.70	70.13	32.31	0.0316	31.773
	HF	79.93	9.54	10.36	71.04	33.64	0.0309	32.281
	DRY	77.54	7.90	7.45	66.81	32.31	0.0338	29.722
Const. disp.	LF	75.68	9.34	9.90	60.86	29.15	0.0336	30.057
	HF	76.89	9.44	10.91	62.43	31.36	0.0325	30.972
	DRY	73.39	7.05	6.11	54.57	29.15	0.0383	26.656

Abbreviations: Const.—constant; disp.—displacement; LF—low frequency (communicating pores); HF—high frequency (isolated pores); Compres.—compressibility (in 1/GPa); CDBM—constant displacement bulk modulus (in GPa); C_{11}–C_{44} are elastic constants (in GPa).

are affected by the compliant pores more than by the stiff pores, the composite with communicating pores exhibits more compliant behaviour in comparison with the same composite with isolated pores.

- The elastic constants estimated under the constant load conditions are significantly higher than those under the constant displacement condition. As stated earlier, the formulations given above are valid only for dilute pore concentrations because the interactions between pores are ignored. In the case of isolated pores, Nishizawa (1982) has shown that the former provides a higher bound for the effective elastic moduli and the latter provides a lower bound. More accurate results may be obtained by incorporating the DEM scheme into the model.

  A numerical calculation has been performed to investigate how the DEM scheme handles this problem. In this numerical simulation, the first group of pores are assumed to be randomly oriented and the second have a preferred orientation with a Gaussian distribution having a standard deviation of 30°. The pore aspect ratio is further assumed to be 0.12 for the first group and 0.03 for the second. Other parameters are kept unchanged. (Hereafter, these parameters will be applied to all following numerical calculations unless otherwise indicated.) Velocity dispersions (defined as $(V^{iso} - V^{com})/V^{iso}$) for P and S waves travelling parallel to the symmetry axis were calculated. The results in Fig. 1 clearly show the velocity dispersion estimated under the constant load condition is much lower than that estimated under the constant displacement condition. Incorporating the DEM scheme with an iteration number equal to 1000, the model provides nearly identical results regardless of the applied boundary condition.
- For perfectly aligned pores, it is observed that

$$C_{44}^{iso} = C_{44}^{com} = C_{44}^{dry} \tag{40}$$

indicating that C_{44} is independent of pore fluid, regardless of the degree of pore fluid communication. This phenomenon has not been reported by O'Connell and Budiansky (1977) or Endres and Knight (1997), since their formulations can handle the randomly-oriented pore system only.

If the pores are not perfectly aligned, C_{44}^{iso} is generally not equal to C_{44}^{com} but C_{44}^{com} is always identical to C_{44}^{dry}. This indicates that the deformation of a solid containing isolated pores involves both shear and dilatation when a pure shear is applied at infinity, resulting

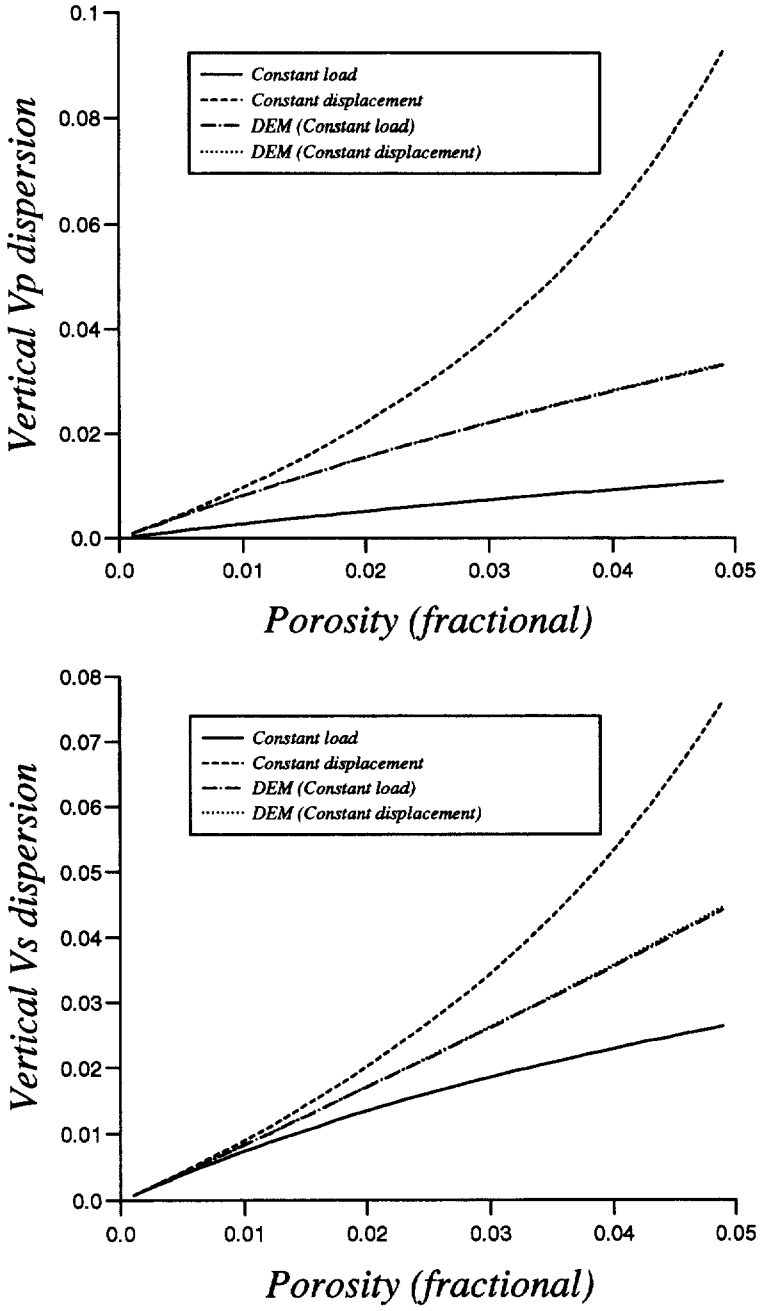

Fig. 1. Comparison of velocity dispersions calculated using various schemes as a function of porosity. Upper: vertical P wave, lower: vertical S wave. Solid line: non-interacting constant load, dashed line: non-interacting constant displacement, dot–dashed line: DEM under the condition of constant load, dotted line: DEM under the condition of constant displacement.

in a fluid-dependent shear modulus. In the communicating pore system, the overall shear stresses are decoupled from the compressional stresses. As a result, no dilatation is caused by applying a pure shear at infinity. The shear modulus of a communicating system is therefore identical to that for dry rocks, independent of the pore fluid properties. Similar results for a solid containing randomly oriented pores have been reported by Endres and Knight (1997).

- It has been reported (e.g. Endres and Knight, 1997; Ravalec and Gueguen, 1996) that the volumetric compressibility of a composite should be independent of pore orientation. The results presented here show that this is true for the constant load condition. Under

the condition of constant displacement, however, the calculated compressibilities are found to vary with pore orientation. The constant displacement bulk modulus (defined in Appendix C) of the composite, on the other hand, is found to be independent of the pore orientation. This is understandable, since in the former case the process involves averaging the compliances (from which the compressibility is calculated) whereas in the latter it involves averaging the stiffnesses (from which the constant displacement bulk modulus is calculated). The results also demonstrate that the constant displacement bulk modulus, unlike the conventional bulk modulus which is simply the reciprocal of the compressibility, provides additional information on the elastic behaviour of an anisotropic material.

In addition to the issues discussed above, the following points were also observed during the numerical calculations, although their values are not listed in Table 1.

- In both cases the estimated dry C^{iso} is found to be identical to the estimated dry C^{com}, indicating the self consistency of the formulations.

  According to the model, the state of pore fluid communication is important because it affects pore pressure which in turn controls the elastic behaviour of a porous rock. In the dry case, however, the effect of pore fluid communication vanishes since the pore pressure itself becomes zero. In other words, the model should provide identical results whether the pores are isolated or they are communicating. This can easily be seen by setting C^f in Q^{iso} [eqn (24)] and Q^{com} [eqns (25), (17) and (18)] to zero.
- There is no dispersion observed when pores with a single aspect ratio are assumed to be perfectly aligned.

  This is obvious since pores having the same geometry and orientation should have the same pore pressure when the composite is subjected to a uniform external stress or strain field. Consequently there is no fluid flow among the pores and, hence, no dispersion should be observed. In a special case where the solid is permeated by round pores, the same phenomenon has been reported by Thomsen (1985), Endres and Knight (1997).

In order to demonstrate the effect of the pore fluid communication on seismic anisotropy, *P*- and *S*-wave velocities were calculated as a function of the incident angle. Figure 2 shows the results obtained under the condition of the constant load (left) and those of constant displacement (right). In general, the impact of the applied condition on the estimation of velocities is high in comparison with the velocity variations caused by the pore fluid communication. In particular, the angular dependence of velocities is also affected by the applied boundary condition.

Figure 3 shows the calculated vertical *P*- (upper) and *S*-wave (lower) velocity dispersions as a function of the concentration of the compliant pores (normalized by the total pore space). The results demonstrate a combined effect of pore shape and pore orientation on the poroelasticity. In two special cases where the concentration of the compliant pores approaches zero or one (i.e. all the pores now have the same shape), the resultant dispersions can only be attributed to the effect of pore orientation.

7. COMPARISON WITH BIOT–GASSMANN'S THEORY

The BG theory has been widely used in the oil industry for estimating velocity dispersion and fluid substitution. The BG theory considers the effect of the macro fluid flow (at the scale of the mean wavelength) on velocity dispersion, whereas this model considers the effect of the local flow (or squirt flow) on velocity dispersion. For a rock containing perfectly aligned pores with a single aspect ratio, this model predicts no velocity dispersion but the BG model does. Even if the pore compressibility is the same everywhere in the system, macro fluid flow can be generated by a passing wave. In any case, the high-frequency velocities predicted by the two models are different.

At the low frequency limit, however, both the IBAPM and BG models make the same assumption about the pore pressure relaxation. The low-frequency version (communicating

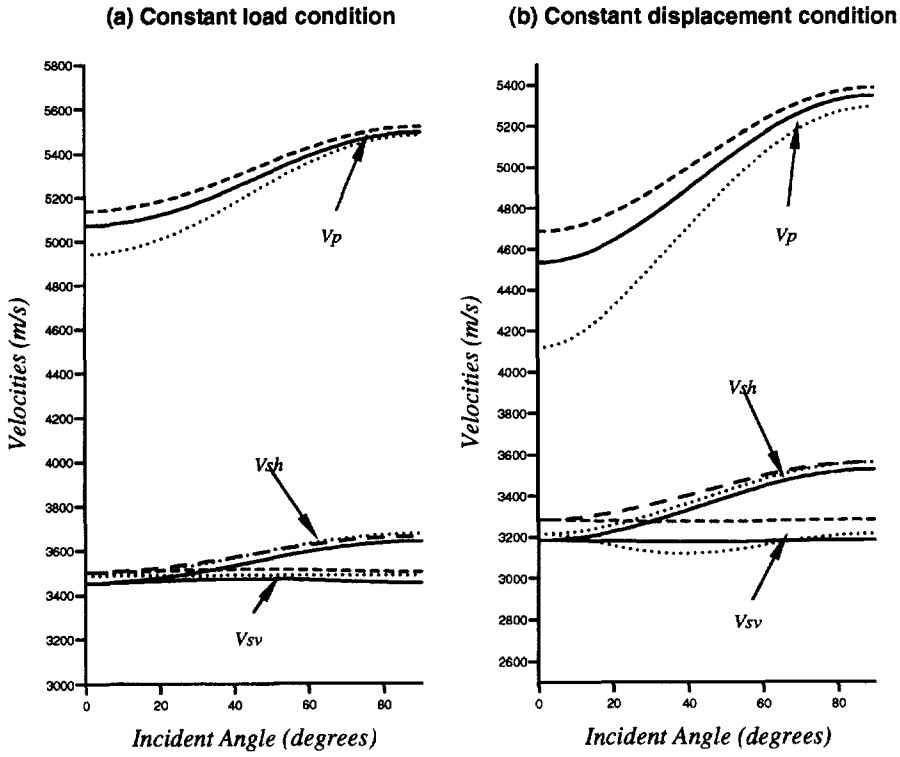

Fig. 2. Illustration of P- and S-wave velocities calculated under the conditions of constant load (upper) and constant displacement (lower) displacement as a function of the incident angle. Dotted lines: dry, solid lines: low-frequency (communicating pores), dashed lines: high-frequency (isolated pores).

pores) of the IBAPM should, therefore, be consistent with the BG theory and its extensions (e.g. Brown and Korringa, 1975).

To be consistent with the BG model, two criteria must be satisfied (Thomsen, 1985): (1) the shear modulus of an unsaturated rock is identical to that of the same rock saturated with liquid, and (2) the unsaturated bulk modulus differs from the saturated bulk modulus by a defined amount predicted by the BG theory (Brown and Korringa in the anisotropic case). In the previous section it has been shown that the non-interacting shear modulus of the communicating system is identical to the dry shear modulus regardless of the condition applied. In this sense the model is consistent with the BG model. In this section more theoretical analysis and numerical examples will be given to show the relationship between the IBAPM and the BG model.

As stated earlier, the IBAPM offers two means of estimating the low-frequency effective elastic constants: one corresponding to the condition of constant load and the other to the condition of constant displacement. The formulations given by Brown and Korringa (1975) and Gassmann (1951) are based on the condition of applied constant load only. I shall, therefore, start with the comparison of the constant load formulation of the model discussed here with that given by Brown and Korringa (1975).

Since eqn (20) is valid for any applied stress σ^0, it may be rewritten as

$$A^*\sigma^0 = A\sigma^0 + \sum_{n=1}^{N} v_n \varepsilon^*_{\text{com}} \tag{41}$$

Substituting eqn (9) into eqn (41) and adding $A\bar{P} - A\bar{P}$, we have

$$A^*\sigma^0 = A\bar{P} - \left\{A - \sum_{n=1}^{N} v_n [C(S-I)]^{-1}\right\}(\bar{P} - \sigma^0) \tag{42}$$

Note that pore stresses $\bar{P}_{ij}$ can be expressed in terms of pore pressure p_f using eqn (14)

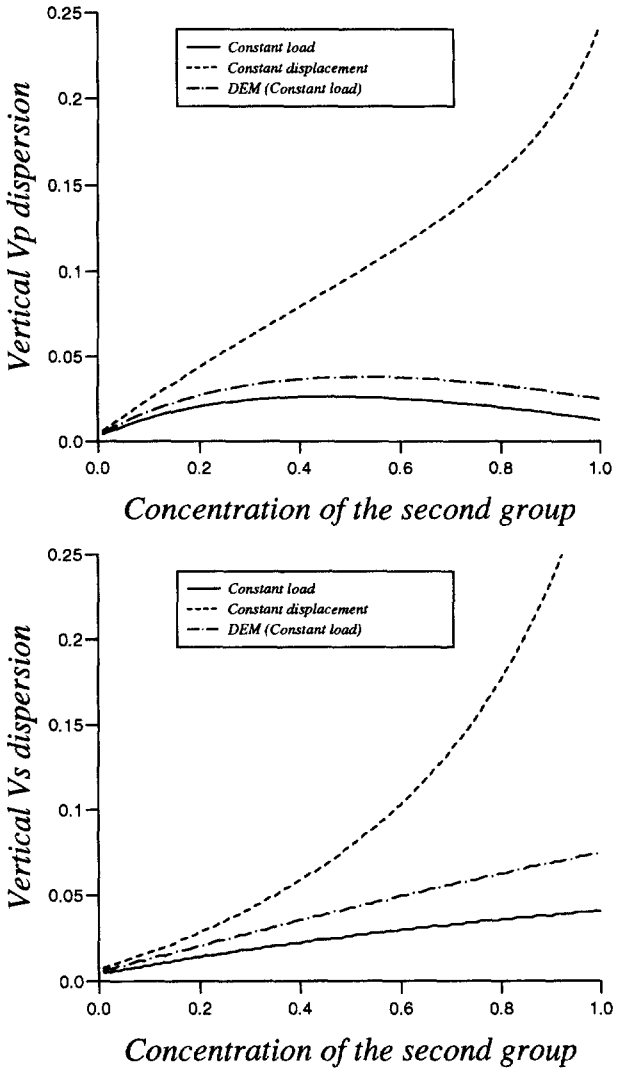

Fig. 3. Illustration of the vertical *P*- (upper) and *S*-wave (lower) velocity dispersions as a function of the concentration of second group of pores (normalized by the total pore space).

(Brown and Korringa, 1975). Also the effective elastic compliances of the dry rockframe can be obtained by setting C^I in eqns (24) to zero

$$A^{\text{dry}} = A - \sum_{n=1}^{N} v_n [C(S-I)]^{-1} \tag{43}$$

Substituting eqns (14) and (43) into eqn (42) and changing the matrices back to tensors, we have

$$A^*_{ijkl}\sigma^0_{kl} = A^{\text{dry}}_{ijkl}(\sigma^0_{kl} + p_f\delta_{kl}) - p_f A_{ijkl}\delta_{kl} \tag{44}$$

Equation (44) is exactly the same as eqn (22) in the Brown–Korringa paper (1975), from which they derived their anisotropic Gassmann equation. This indicates that our non-interacting formulation under the condition of the constant load is strictly consistent with that of Brown–Korringa. The difference between the two models is that they express the pore volume change ΔV_p as a function of the dry rockframe moduli and the bulk modulus

of the pore fluid, while the IBAPM evaluates ΔV_p from the specified pore shape parameters and pore fluid properties [eqns (10)–(14)].

Numerical studies have been carried out to check the consistency of the IBAPM with the Brown–Korringa model. The effective elastic constants of porous rock with communicating pores are firstly calculated using IBAPM under the two specified conditions. The same pore parameters are used to calculate the elastic constant of the dry rockframe by simply setting C' to zero. The Brown–Korringa equation is then used to calculate the effective elastic constants of the saturated rock from the dry rockframe moduli calculated above and the same pore fluid properties.

Figure 4 shows $C_{33}^{\text{wet}} - C_{33}^{\text{dry}}$ as a function of porosity. Note that at the low frequency limit the non-interacting formulation of IBAPM under the condition of constant load (dashed line) gives results identical to that of BG (dotted line), confirming the mathematical verifications above.

However, under the condition of constant displacement, the dependence of the elastic moduli on pore fluid predicted by the IBAPM (dot–dashed line) is much higher than the Brown–Korringa prediction. Incorporating the DEM scheme into the constant load formulation provides results inconsistent with the Brown–Korringa prediction, but nicely lying between the two extremes predicted by IBAPM under the two conditions.

Figure 5 further shows the elastic constant C_{44} as a function of the fluid bulk modulus. As observed earlier, the non-interacting C_{44}^{com} was found to be independent of the bulk modulus of the pore fluid, regardless of the applied boundary condition. It also shows that the dispersion predicted under the condition of constant load is much smaller than that of constant displacement. Again, it was found that both the absolute value of C_{44} approximated

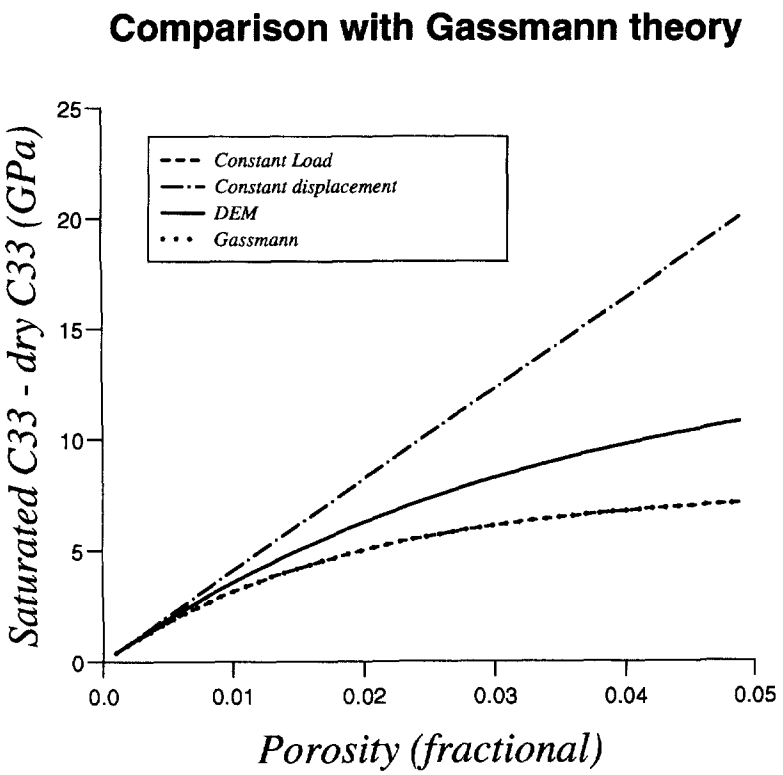

Fig. 4. Comparison of the dependencies of the elastic constant C_{33} on pore fluid calculated using various schemes. Dashed line: non-interacting constant load, dot–dashed line: non-interacting constant displacement, solid line: DEM under the condition of constant load, dotted line: anisotropic Gassmann (Brown and Korringa, 1975).

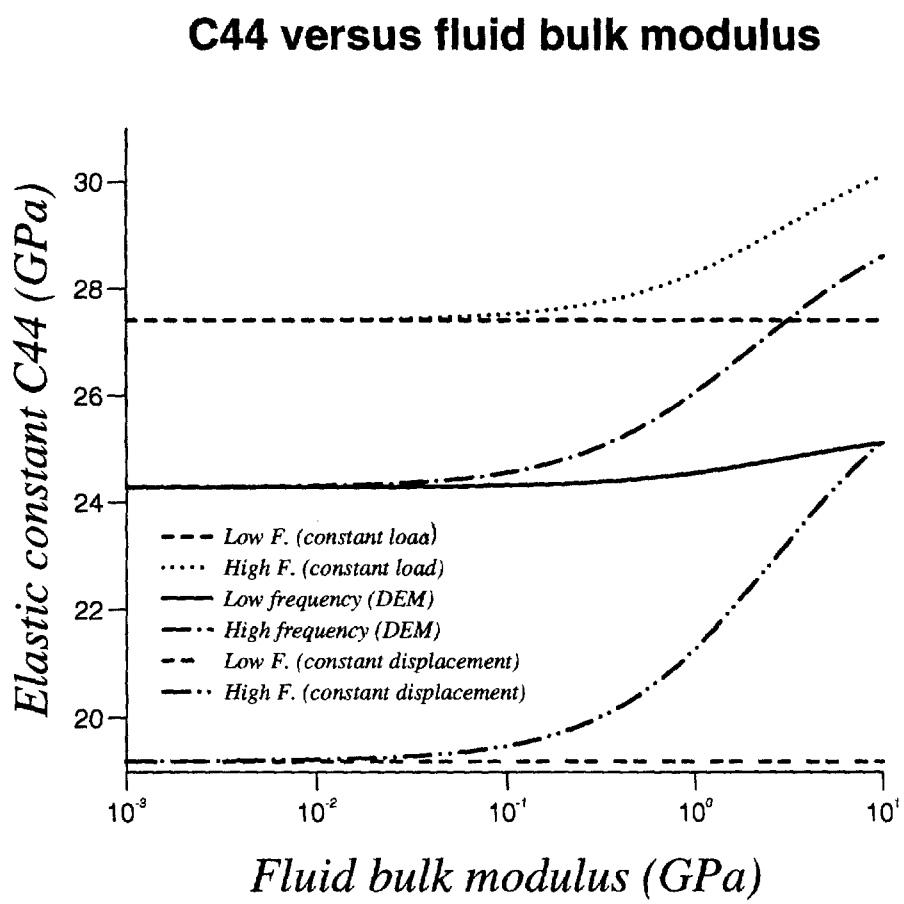

Fig. 5. Comparison of the low- and high-frequency elastic constant C_{44} as a function of the bulk modulus of pore fluid.

by DEM and its dispersion lie within the two extremes mentioned above. However the low-frequency C_{44} from the DEM exhibits a slight dependence on the bulk modulus of the pore fluid.

The inconsistency of the SC or DEM with the BG theory has been observed by a number of authors (e.g. Thomsen, 1985; Berryman, 1992; Endres and Knight, 1997). The inconsistency is interpreted as a result of violating the BG basic assumption of equalised pore pressure by SC and DEM. Although the pore pressure during each iteration is kept the same by DEM, it varies from iteration to iteration, due to the change of the elastic constants of the host medium. Thomsen (1985) believes that the BG theory adequately describes the dependence of elastic moduli on pore fluid compressibility at low frequencies. Thomsen (1985) and Berryman (1992) have proposed methods to overcome the violation of the BG relationship by the SC and DEM schemes.

8. APPLICATION TO LABORATORY MEASUREMENTS

Rathore *et al.* (1995) developed a technique for manufacturing artificial porous rocks permeated with parallel cracks with known geometries. Porous rock samples were constructed by cementing together the sand grains using an epoxy resin. Metal disks with known positions, orientations, shape and aspect ratio were embedded into the artificial samples during the construction process. These disks were later leached out chemically, leaving disk voids representing a network of parallel cracks sitting in a porous rock. Two rock samples were manufactured during their experiment: one containing parallel cracks

Table 2. Crack parameters

Crack shape	circular
Crack diameter	5.50 mm
Crack thickness	0.02 mm
Crack density	0.10
Number of cracks in 0.001 m^3	4808
Number of layers	48

and the other being a crack-free dummy. Table 2 shows the designed parameters for the cracks. Ultrasonic velocities V_P, V_{SV} and V_{SH} were measured at eight angles to the symmetry axis of the cracks with a 22.5° increment.

Parameters used by Rathore *et al.* (1995) were adopted in simulating the laboratory measurements. The solid grains are assumed to have a bulk modulus of 18.2 GPa, a shear modulus of 10.2 GPa and a density of 2.08 g/cm^3. The bulk modulus of the pore fluid is assumed to be 2.25 GPa and a density of 1 g/cm^3. The total pore space comprises two parts: equant inter-granular pores with a porosity of 34.6% and cracks with a porosity of 0.23%. The equant pores are assumed to be randomly oriented, giving an isotropic porous matrix. Their aspect ratio (0.25) was derived by fitting the predictions to *P*- and *S*-wave velocities of the dummy sample. The aspect ratio for the cracks (0.0036) was calculated from the crack parameters.

Figure 6 compares the predictions with the measured *P*- and *S*-wave velocities of the dry sample as a function of the incident angle. Despite a slight over-estimate in the *S*-wave velocities, the predictions simulate the measurements rather well.

Figure 7 compares the measurements with the low-frequency (solid lines) and high-frequency (dashed lines) predictions. The results clearly show that the low-frequency version simulates the laboratory measurements much better than its high-frequency counterpart. The low-frequency behaviour of the measurement may be attributed to the relatively large

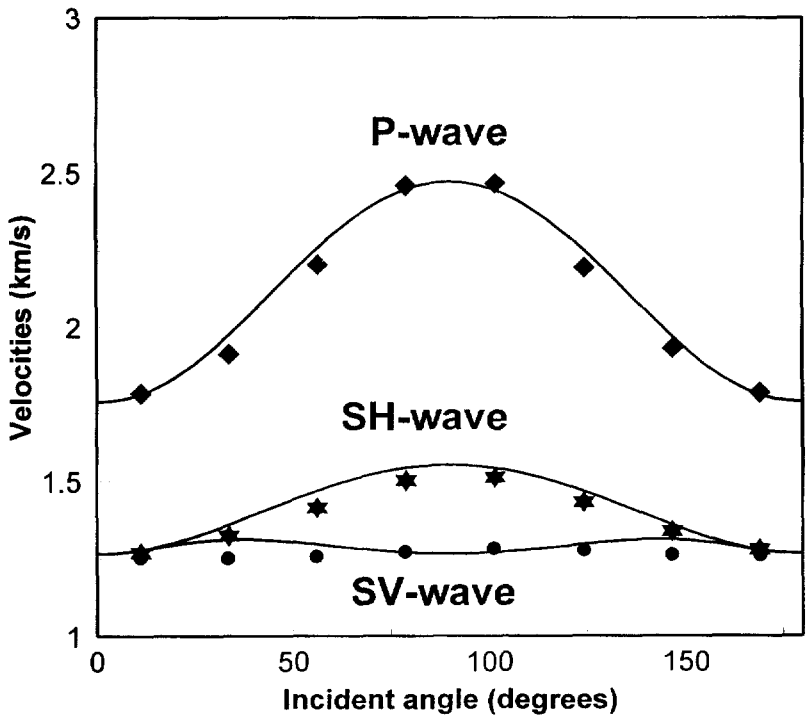

Fig. 6. Comparison of *P*- and *S*-wave velocities measured by Rathore *et al.* (1995) of the dry synthetic sample with aligned cracks and the predictions from the IBAPM.

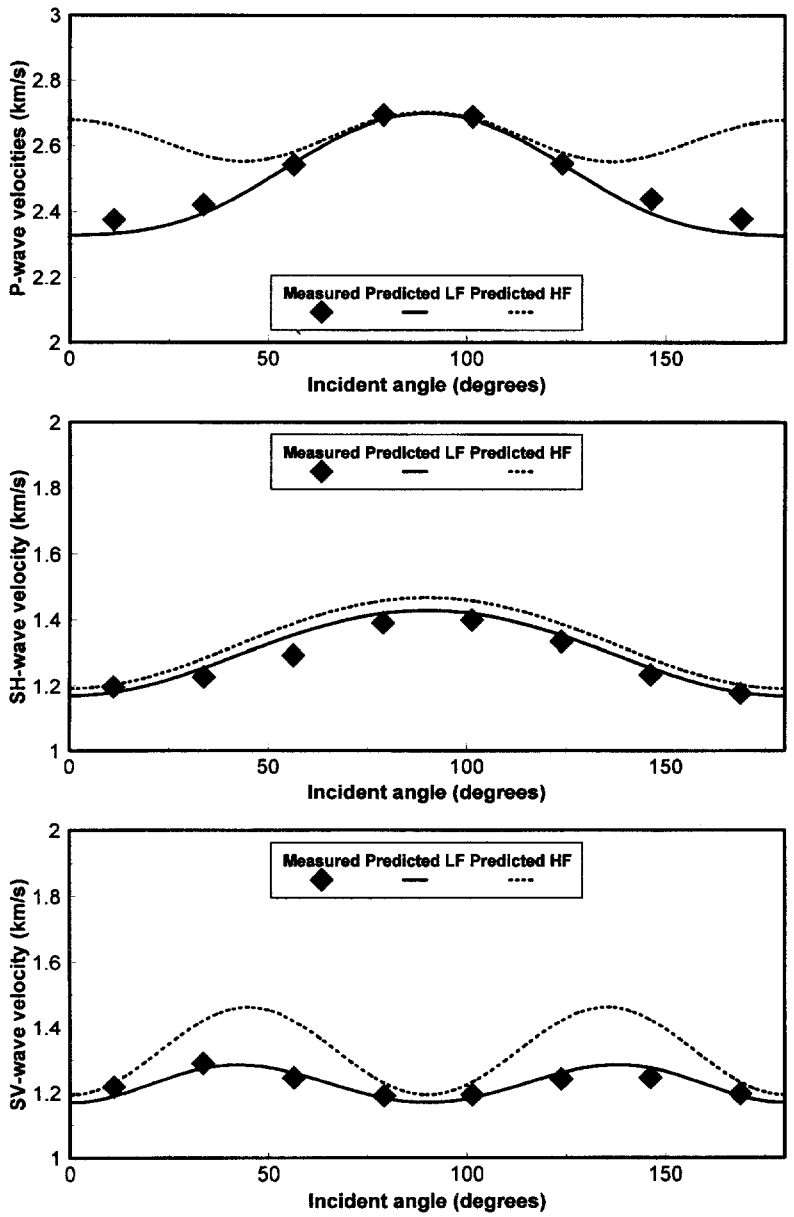

Fig. 7. Comparison of *P*- and *S*-wave velocities of the saturated synthetic sample (Rathore *et al.*, 1995) and IBAPM's low- (solid lines) and high-frequency (dashed lines) predictions.

size of the cracks (5.5 mm in diameter), which greatly enhances the permeability of the synthetic sample.

The main advantage of the inclusion-based poroelasticity models over the traditional ones such as Biot's (1956a, b) is that the former do not require dry frame moduli as the key input parameters. The inclusion-based models calculate the dry moduli from pore parameters (aspect ratios) and the elastic properties of solid and pore fluid. This feature makes the inclusion-based models very practical since in many cases we do not really know the dry frame moduli. The goodness of fit between the measured dry and saturated *P*- and *S*-wave velocities and the predictions demonstrates the predictive power of the model, considering that nearly all the input parameters are defined from the independent measurements.

9. CONCLUSIONS

(1) An inclusion-based anisotropic poroelasticity model (IBAPM) has been developed. The model simulates the low-frequency response of a porous rock by assuming a communicating pore system and the high-frequency response by an isolated pore system.

(2) The local flow within a communicating pore system and, hence, the velocity dispersion are controlled by two key factors: pore geometry and pore orientation. Unlike many other poroelasticity models which use the dry rockframe moduli as input parameters, IBAPM calculates them from pore parameters and properties of the matrix and fluid. This feature makes the model very useful since in many practical applications the dry frame moduli are not measurable.

(3) A further major difference between IBAPM and the previous poroelasticity models is that IBAPM offers two approximations, one corresponding to the condition of constant load and the other to the condition of constant displacement. Numerical results show that velocity dispersion calculated by applying the constant load boundary condition is much lower than that calculated by applying that of constant displacement. Incorporating the DEM theory into IBAPM provides results lying between the two extremes.

(4) The non-interacting constant load formulation of IBAPM is found to be completely consistent with the BG theory. At higher pore concentrations, although DEM violates the BG assumption on the equalised pore pressure, it probably predicts the pore fluid dependence of the elastic moduli more accurately than BG.

(5) The IBAPM has been applied to simulate the laboratory measurement made by Rathore *et al.* (1995). The results clearly show that the low-frequency version simulates the laboratory measurements much better than its high-frequency counterpart. The low-frequency behaviour of the measurements may be attributed to the relative large size of the cracks (5.5 mm in diameter), which greatly enhances the permeability of the synthetic sample.

Acknowledgements—The author is indebted to the sponsors of the London University Research Programme in Seismic Lithology, Amoco (UK) Exploration Company, Elf UK plc, Enterprise Oil plc, Fina Exploration Ltd, Mobil North Sea Ltd and Texaco Britain Ltd, for their support of this research. I especially thank Professors Roy White and Michael King, both from University of London for reviewing the manuscript and many useful discussions. I would also like to thank Dr Leonid Germanovich and an anonymous referee for their constructive review of the manuscript.

REFERENCES

Berryman, J. G. (1992) Single-scattering approximations for coefficients in Biot's equations of poroelasticity. *Journal of Acoustic Society of America* **91,** 551–571.

Biot, M. A. (1956a) Theory of propagation of elastic waves in a fluid saturated porous solid. I. Low-frequency range. *Journal of Acoustic Society of America* **28,** 168–178.

Biot, M. A. (1956b) Theory of propagation of elastic waves in a fluid saturated porous solid. II. Higher-frequency range. *Journal of Acoustic Society of America* **28,** 179–191.

Blangy, J. P., Strandenes, S., Moos, D. and Nur, A. (1993) Ultrasonic velocities in sands—revisited. *Geophysics* **58,** 344–356.

Brown, R. J. S. and Korringa, J. (1975) On the dependence of elastic properties of a porous rock on the compressibility of the pore fluid. *Geophysics* **40,** 608–616.

Bruner, W. M. (1976) Comment on "seismic velocities in dry and saturated cracked solids" by Richard J. O'Connell and Bernard Budiansky. *J. Geophys. Res.* **81,** 2573–2576.

Budiansky, B. (1965) On the elastic moduli of some heterogeneous materials. *Journal of Mechanics and Physics of Solids* **13,** 223–227.

Dutta, N. C. and Odé, H. (1979a) Attenuation and dispersion of compressional wave in fluid-filled rocks with partial gas saturation (White model)—Part I. Biot theory. *Geophysics* **44,** 1777–1788.

Dutta, N. C. and Odé, H. (1979b) Attenuation and dispersion of compressional wave in fluid-filled rocks with partial gas saturation (White model)—Part II. Results. *Geophysics* **44,** 1789–1805.

Endres, A. L. and Knight, R. J. (1997) Incorporating pore geometry and fluid pressure communication into modelling the elastic behavior of porous rocks. *Geophysics* **62,** 106–117.

Eshelby, J. D. (1957) The determination of the elastic field of an ellipsoidal inclusion, and related problems. *Proceedings of the Royal Society of London, Series A* **241,** 376–396.

Gassmann, F. (1951) Elasticity of porous media. *Vierteljahrschrift der Naturforschenden Gesellschaft in Zürich* **96,** 1–21.

Germonovich, L. N. and Dyskin, A. V. (1994a) Virial expansions in problems of effective characteristics. 1. General concepts. *Mech. Composite Mater.* **30,** 157–167.
Germonovich, L. N. and Dyskin, A. V. (1994b) Virial expansions in problems of effective characteristics. 2. Antiplannar deformation of a fiber composite. Analysis of self-consistent methods. *Mech. Composite Mater.* **30,** 234–243.
Gordon, R. B. and Davis, L. A. (1968) Velocity and attenuation of seismic waves in imperfectly elastic rocks. *J. Geophys. Res.* **73,** 3917–3925.
Hashin, Z. and Shtrikman, S. (1963) A variation approach to the theory of the elastic behaviour of multiphase materials. *Journal of Mechanics and Physics of Solids* **11,** 127–140.
Henyey, F. S. and Pomphrey, N. (1982) Self-consistent elastic moduli of a crack solid. *Geophys. Res. Lett.* **9,** 903–906.
Hill, R. (1965) A self-consistent mechanics of composite materials. *Journal of Mechanics and Physics of Solids* **13,** 213–222.
Hoenig, A. (1978) The behaviour of a flat elliptical crack in an anisotropic elastic body. *International Journal of Solids and Structures* **14,** 925–934.
Hoenig, A. (1979) Elastic moduli of the non-randomly cracked body. *International Journal of Solids and Structures* **15,** 137–154.
Hornby, B. E., Schwartz, L. M. and Hudson, J. A. (1994) Anisotropic effective-medium modeling of the elastic properties of shales. *Geophysics* **59,** 1570–1583.
Hudson, J. A. (1981) Wave speed and attenuation of elastic waves in material containing cracks. *Geophys. J. Roy. Astr. Soc.* **64,** 133–150.
Johnston, D. H., Toksöz, M. N. and Timur, A. (1979) Attenuation of seismic waves in dry and saturated rocks. II: Mechanisms. *Geophysics* **44,** 691–711.
Kuster, G. T. and Toksöz, M. N. (1974) Velocity and attenuation of seismic waves in two-phase media. Part 1: Theoretical formulation. *Geophysics* **39,** 587–606.
Lin, S. and Mura, T. (1973) Elastic fields of inclusions in anisotropic media. *Phys. Status Solidi* **(a)15,** 281–285.
Mavko, G. and Jizba, D. (1991) Estimating grain-scale fluid effects on velocity dispersion in rocks. *Geophysics* **56,** 1940–1949.
Mavko, G. and Jizba, D. (1994) Relation between seismic *P*- and *S*-wave velocity dispersion in saturated rocks. *Geophysics* **59,** 87–92.
Mavko, G. and Nur, A. (1975) Melt squirt in the asthenosphere. *J. Geophys. Res.* **80,** 1444–1448.
Mavko, G. and Nur, A. (1975) Wave attenuation in partially saturated rocks. *Geophysics* **44,** 161–178.
Mukerji, T. and Mavko, G. (1994) Pore fluid effects on seismic velocity in anisotropic rocks. *Geophysics* **59,** 233–244.
Mura, T. (1987) *Micromechanics of Defects in Solids.* Martinus Nijhoff, Dordrecht.
Nishizawa, O. (1982) Seismic velocity anisotropy in a medium containing oriented cracks—transversely isotropic case. *J. Phys. Earth* **30,** 331–347.
O'Connell, R. J. and Budiansky, B. (1977) Viscoelastic properties of fluid-saturated cracked solids. *J. Geophys. Res.* **82,** 5719–5736.
Rathore, J. S., Ejaer, E., Holt, R. M. and Renlie, L. (1995) *P*- and *S*-wave anisotropy of a synthetic sandstone with controlled crack geometry. *Geophys. Prosp.* **43,** 711–728.
Ravalec, M. L. and Guéguen, Y. (1996) High- and low-frequency elastic moduli for saturated porous/cracked rock-differential self-consistent and poroelastic theories. *Geophysics* **61,** 1080–1094.
Shams, M. K., King, M. S. and Worthington, M. H. (1993) Whitchester seismic cross-hole test site—petrophysical studies of cores. In *Expanded Abstracts 55th EAGE Mtg.* Stanvanger, Norway.
Sheng, P. (1991) Consistent modeling of the electrical and elastic properties of sedimentary rocks. *Geophysics* **56,** 1236–1243.
Thomsen, L. (1985) Biot-consistent elastic moduli of porous rocks: low-frequency limit. *Geophysics* **50,** 2797–2807.
Thomsen, L. (1995) Elastic anistropy due to aligned cracks in porous rocks. *Geophys. Prosp.* **43,** 805–829.
Toksöz, M. N., Johnston, D. H. and Timur, A. (1979) Attenuation of seismic waves in dry and saturated rocks: I. Laboratory measurements. *Geophysics* **44,** 681–690.
Walsh, J. B. (1966) Seismic attenuation in rock due to friction. *J. Geophys. Res.* **71,** 2591–2599.
White, J. E. (1975) Computed seismic speeds and attenuation in rocks with partial gas saturation. *Geophysics* **40,** 224–232.
Winkler, K. W. and Nur, A. (1982) Seismic attenuation: effects of pore fluids and frictional sliding. *Geophysics* **47,** 1–15.
Willis, J. R. (1977) Bounds and self-consistent estimates for the overall properties of anisotropic composite. *Journal of Mechanics and Physics of Solids* **25,** 185–202.
Wyllie, M. R. J., Gardner, G. H. F. and Gregory, A. R. (1962) Studies of elastic wave attenuation in porous media. *Geophysics* **27,** 569–589.
Xu, S. and White, R. E. (1995a) A new velocity model for clay-sand mixtures. *Geophys. Prosp.* **43,** 91–118.
Xu, S. and White, R. E. (1995b) Poro-elasticity of clastic rocks: a unified model. In *Trans. 36th Ann. SPWLA Symp.*, Paris, Paper V.
Xu, S. and White, R. E. (1996) A physical model for shear-wave velocity prediction. *Geophys. Prosp.* **44,** 687–717.

APPENDIX A: ESHELBY TENSOR S_{ijkl} FOR A PORE IN A HEXAGONAL SOLID

Lin and Mura (1973) and Mura (1987) have shown how to calculate the Eshelby tensor S_{ijkl} for a pore embedded in a solid with hexagonal symmetry.

$$S_{ijmn} = \frac{1}{8\pi}(G_{ipjq} + G_{jpiq})C_{pqmn} \tag{45}$$

where C is the stiffness tensor of the solid. G is a four-rank geometry tensor which depends on the pore shape and the elastic properties of the solid. For an oblate spheroidal pore with an aspect ratio $\alpha = c/a$, Lin and Mura (1973) claim that there are 12 non-zero elements for G_{ijkl} which can be calculated using the following integrals.

$$G_{1111} = \frac{\pi}{2}\int_0^1 (1-x^2)[(f(1-x^2)+h\rho^2x^2)((3e+d)(1-x^2)+4f\rho^2x^2)-g^2\rho^2(1-x^2)x^2]\Delta\,dx \tag{46}$$

$$G_{2222} = G_{1111} \tag{47}$$

$$G_{3333} = 4\pi\int_0^1 x^2\rho^2(d(1-x^2)+f\rho^2x^2)(e(1-x^2)+f\rho^2x^2)\Delta\,dx \tag{48}$$

$$G_{1122} = \frac{\pi}{2}\int_0^1 (1-x^2)[(f(1-x^2)+h\rho^2x^2)((e+3d)(1-x^2)+4f\rho^2x^2)-3g^2\rho^2(1-x^2)x^2]\Delta\,dx \tag{49}$$

$$G_{2211} = G_{1122} \tag{50}$$

$$G_{1133} = 2\pi\int_0^1 x^2\rho^2[((d+e)(1-x^2)+2f\rho^2x^2)(f(1-x^2)+h\rho^2x^2)-g^2\rho^2(1-x^2)x^2]\Delta\,dx \tag{51}$$

$$G_{2233} = G_{1133} \tag{52}$$

$$G_{3311} = 2\pi\int_0^1 (1-x^2)(d(1-x^2)+f\rho^2x^2)(e(1-x^2)+f\rho^2x^2)\Delta\,dx \tag{53}$$

$$G_{3322} = G_{3311} \tag{54}$$

$$G_{1212} = \frac{\pi}{2}\int_0^1 (1-x^2)^2[g^2x^2\rho^2-(d-e)(f(1-x^2)+h\rho^2x^2)]\Delta\,dx \tag{55}$$

$$G_{1313} = -2\pi\int_0^1 (1-x^2)x^2\rho^2(e(1-x^2)+f\rho^2x^2)\Delta\,dx \tag{56}$$

$$G_{2323} = G_{1313} \tag{57}$$

where

$$\begin{aligned}
\Delta &= \{[e(1-x^2)+f\rho^2x^2][(d(1-x^2)+f\rho^2x^2)(f(1-x^2)+h\rho^2x^2)-g^2\rho^2(1-x^2)x^2]\}^{-1}\\
d &= C_{1111}\\
e &= (C_{1111}-C_{1122})/2\\
f &= C_{2323}\\
g &= C_{1133}+C_{2323}\\
h &= C_{3333}\\
\rho^2 &= (1/\alpha^2)
\end{aligned} \tag{58}$$

APPENDIX B: CONVERTING TENSORS TO MATRICES

Following the notations given by Hill (1965), a 9×1 column vector is used to represent a second-rank tensor, e.g. e and σ, and a 9×9 matrix to represent a fourth-rank tensor, e.g. A and C. The tensor components are arranged using the following sequence: $11 \Rightarrow 1$, $22 \Rightarrow 2$, $33 \Rightarrow 3$, $23 \Rightarrow 4$, $13 \Rightarrow 5$, $12 \Rightarrow 6$, $32 \Rightarrow 7$, $31 \Rightarrow 8$, and $21 \Rightarrow 9$. The leading pair of indices corresponds to rows and the terminal pair to columns so that the inner product of tensor $A_{ijkl}e_{kl}$ can be written as Ae. Similarly $A_{ijkl}C_{klmn}$ can be written as AC and $A_{ijkl}C_{klmn}e_{mn}$ as ACe.

The inverse of a fourth-rank tensor A is defined as (Hill, 1965; Hornby *et al.*, 1994)

$$AA^{-1} = A^{-1}A = I \tag{59}$$

where A^{-1} is the inverse of tensor A and I is a unit tensor

$$I_{ijkl} = \tfrac{1}{2}(\delta_{ik}\delta_{jl} + \delta_{il}\delta_{jk}) \tag{60}$$

and δ_{ij} is the Kronecker delta.

All the fourth-rank tensors we deal with in this paper have the following symmetry

$$A_{ijkl} = A_{jikl} = A_{ijlk} \tag{61}$$

Their corresponding matrices are consequently singular with a rank less than or equal to six.

APPENDIX C: COMPRESSIBILITY AND BULK MODULUS OF AN ANISOTROPIC MEDIUM

The compressibility of an isotropic medium is defined as the ratio of the normalized bulk volume change to the applied hydrostatic stress

$$c = \frac{\dfrac{\Delta V}{V}}{\sigma_0} \tag{62}$$

where $\Delta V/V$ denotes the normalized bulk volume change in the elementary volume V, which is a function of the total strain e,

$$\frac{\Delta V}{V} = e_x + e_y + e_z \tag{63}$$

and σ_0 is the applied hydrostatic stress with

$$\sigma_x = \sigma_y = \sigma_z = \sigma_0 \tag{64}$$

The definition of the bulk modulus is the inverse of the compressibility, i.e. the ratio of the hydrostatic stress to the normalized bulk volume change (dilatation) under simple hydrostatic pressure,

$$k = \frac{\sigma_0}{\dfrac{\Delta V}{V}} \tag{65}$$

The definition of the compressibility [eqn (62)] and that of the bulk modulus [eqn (65)] can be applied to the anisotropic case without modification. Assuming the rock has a compliance tensor A, the normalized volume change due to the applied hydrostatic stress σ_0 is

$$\frac{\Delta V}{V} = A_{11}\sigma_x + A_{12}\sigma_y + A_{13}\sigma_z + A_{21}\sigma_x + A_{22}\sigma_y + A_{23}\sigma_z + A_{31}\sigma_x + A_{32}\sigma_y + A_{33}\sigma_z \tag{66}$$

Since $\sigma_x = \sigma_y = \sigma_z = \sigma_0$, the compressibility for an anisotropic medium is given by

$$c = \sum_{i=1}^{3}\sum_{j=1}^{3} A_{ij} \tag{67}$$

Equation (67) is exactly the same as the definition of the compressibility given by Brown and Korringa (1975).

Since the bulk modulus is defined under the condition of constant load with $\sigma_x = \sigma_y = \sigma_z = \sigma_0$, it may be referred to as the constant load bulk modulus (CLBM). The CLBM for an anisotropic medium is always the reciprocal of the compressibility and consequently carries no more information on the elastic behaviour of the material than does the compressibility. A new bulk modulus is defined as the ratio of the average stress σ_0 to the normalized bulk volume change as the material undergoes a uniform volume deformation with

$$e_x = e_y = e_z = e_0 \tag{68}$$

Mathematically, the new bulk modulus has the same form as eqn (65). But σ_0 now denotes the average stress of σ_x, σ_y and σ_z, i.e.

$$\sigma_0 = \tfrac{1}{3}(\sigma_x + \sigma_y + \sigma_z) \tag{69}$$

Under the condition of uniform volume deformation as specified by eqn (68), the normalized volume change is given by

$$\frac{\Delta V}{V} = e_x + e_y + e_z = 3e_0 \tag{70}$$

Since the new bulk modulus is defined under the condition of constant strain, it may be referred to as the constant displacement bulk modulus (CDBM). Applying Hooke's law, the constant displacement bulk modulus for an anisotropic medium can be expressed as a function of the elastic constants

$$k = \frac{1}{9} \sum_{i=1}^{3} \sum_{j=1}^{3} C_{ij} \tag{71}$$

where C is the stiffness tensor of the material.

It should be borne in mind that the constant displacement bulk modulus defined above is generally not the reciprocal of the compressibility. Unlike the CLBK it provides extra information about the elastic behaviour of an anisotropic material. However, in the isotropic case, the CDBM is exactly the same as the conventional bulk modulus CLBK. This is understandable because, in an isotropic material, eqn (68) still holds when a hydrostatic pressure applies [eqn(64)] and vice versa.